

## SUPPLEMENTARY INFORMATION

### Microfluidic Chemotaxis Platform for Differentiating the Roles of Soluble and Bound Amyloid- $\beta$ on Microglial Accumulation

5 Hansang Cho<sup>1</sup>, Tadafumi Hashimoto<sup>2</sup>, Elisabeth Wong<sup>1</sup>, Yukiko Hori<sup>2</sup>, Levi B. Wood<sup>3</sup>  
Lingzhi Zhao<sup>2</sup>, Kevin M. Haigis<sup>3</sup>, Bradley T. Hyman<sup>2</sup>, Daniel Irimia<sup>1\*</sup>

<sup>1</sup>BioMEMS Resource Center, Massachusetts General Hospital, Harvard Medical School

<sup>2</sup>MassGeneral Institute for Neurodegenerative Disease, Massachusetts General Hospital,  
Harvard Medical School

10 <sup>3</sup>Molecular Pathology Unit, Massachusetts General Hospital, Harvard Medical School

## Supplementary Results

**Physical stability of  $A\beta$  gradients.** To validate the physical stability of gradients, we monitored the intensity changes of FITC-conjugated soluble amyloid- $\beta$  ( $A\beta$ ) for 9 days. On 'day 0',  $sA\beta$  solutions at  $2.3 \mu\text{g.mL}^{-1}$  were added to the central reservoir and culturing medium to the two side reservoirs (**Fig. S1a**). Even though we used  $sA\beta$  of  $230 \text{ ng.mL}^{-1}$  as the maximum value in cell experiments, we used FITC-labeled  $A\beta$  of 10 times higher than the maximum value in the diffusion experiment to effectively monitor the weak signals of  $A\beta$  gradients, which was challenging with  $A\beta$  in a physiological range. The microfluidic platform was imaged every two days, and then fluorescent signals were normalized with respect to the maximum intensity on each day. In Figure S1, we quantified the degradation of gradients by measuring the intensity in the side reservoirs,  $I_{4.6}$  (at a radius of 4.6 mm from the center position) compared to the intensity in the central reservoir at a maximum,  $I_0$  (at a radius of 0 mm). We observed that approximately 90% of the original monomeric  $sA\beta$  gradients (**Fig. S1b - c**) and 95 % of oligomeric  $sA\beta$  gradients (**Fig. S1b, d**) were preserved for 9 days. The better stability of oligomeric  $sA\beta$  is probably due to the higher molecular weight of  $sA\beta$  and consequently to slower diffusion.

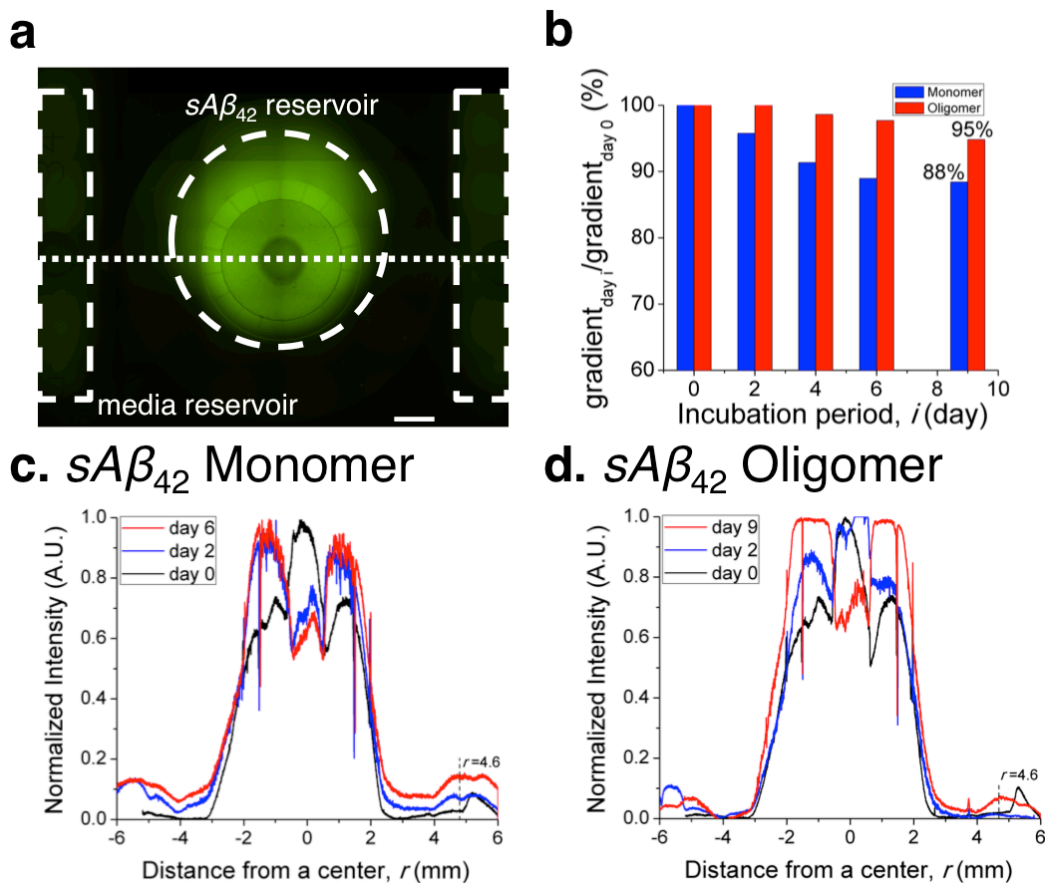


**Figure S1. Verification of the physical stability of soluble  $A\beta$ .** **a**, The gradients of soluble  $A\beta$  is visualized by using a FITC-conjugated  $A\beta$ . **b**, By 9 days, gradients of monomeric and oligomeric  $A\beta$  remain at 88 and 95 % of the original values. The intensity profiles present a slight degradation of the gradients over time (**c**, **d**). Scale bar, 1 mm.

30 **Chemical stability of  $A\beta$ .** The stability of  $A\beta$  was investigated with regard to degradation or aggregation in the cell culture solutions used in the experiments. Measurements were performed by ELISA, western blot, and EM imaging, for incubation times of up to 2 days (**Fig. S2**).

To check for any loss or degradation of  $A\beta$  over time, the total amounts of  $A\beta$  were  
35 measured with an ELISA kit for any forms of  $A\beta$  (**Fig. S2a**). The higher decrease rate of the  
total amounts in  $A\beta$  monomeric solutions is probably due to lower stability of  $A\beta$  monomers  
and their degradation into smaller fragments faster than  $A\beta$  oligomers over time.

In order to evaluate the stability of  $A\beta$  monomers against further aggregation and  $A\beta$  fibrils  
against degradation forming  $A\beta$  oligomers over time, the amounts of  $A\beta$  oligomers were  
40 quantified with an ELISA kit specific for  $A\beta$  oligomers. The  $A\beta$  oligomers detected from  
 $A\beta$  monomeric solutions of  $230 \text{ ng.mL}^{-1}$  in total were only 0.67% and 0.15% by weight in  
fresh and incubating media, respectively. Also,  $A\beta$  oligomers from  $A\beta$  fibrillar solutions  
were below the low detection limit of the kit in both fresh and incubating media (**Fig. S2c**).  
Based on these measurements, the  $A\beta$  monomers and fibrils were regarded as stable during  
45 the two days cell experiments.

To evaluate the stability of  $A\beta$  oligomers with regard to aggregation into  $A\beta$  fibrils, we  
compared the amounts of oligomers with the ELISA kit specific for  $A\beta$  oligomer and  
imaged fibrils with electron microscopy (EM). The measured  $A\beta$  oligomers from  $A\beta$   
oligomeric solutions of  $230 \text{ ng.mL}^{-1}$  in total were 9.5% and 5.6% by weight in fresh and  
50 incubating media, respectively (**Fig. S2b**); no fibrils were found from EM imaging of the  
oligomeric solutions (**Fig. S2c**). Based on these measurements, we estimated that the  
fraction of higher molecular weight oligomers almost doubled but remained in an  
oligomeric form, confirmed by the WB results showing slight aggregation of  $A\beta$  oligomers  
(**Fig. S2d**). (Student's t-test. \*  $P < 0.001$  with respect to  $A\beta$  oligomers on the same day,  $n =$   
55 4 for each condition. Data represent mean  $\pm$  s.e.m.)

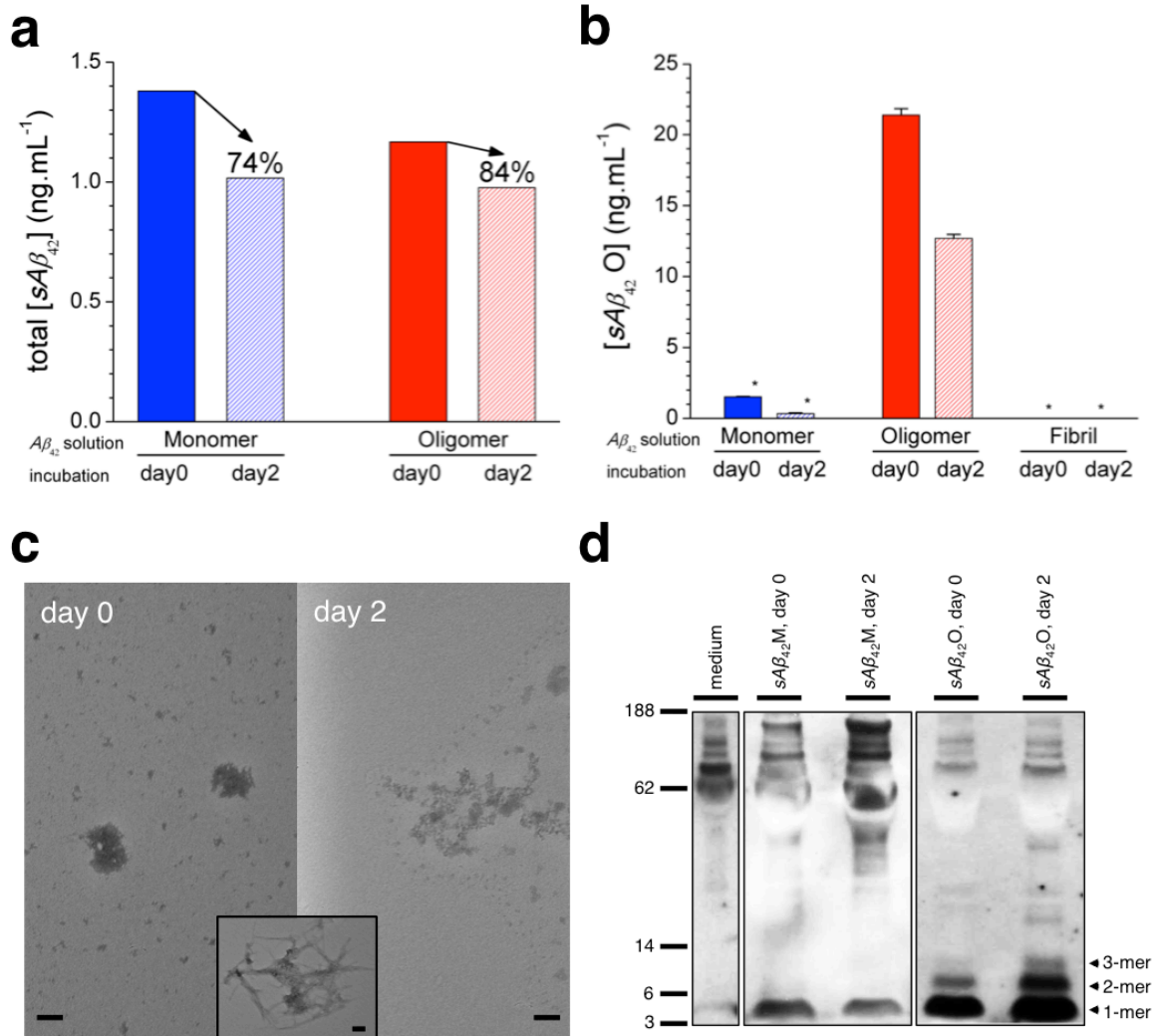


**Figure S2. Verification of the chemical stability of soluble  $A\beta$ .** **a**, Over 70 % of soluble  $A\beta$  in a total mass remains against degradation in culture medium. Small amounts of aggregation may be induced; we maintained most of the original forms. This is validated by measuring oligomeric  $A\beta$  using an oligomer-specific ELISA kit (**b**) and EM imaging of oligomeric  $A\beta$  (**c**), and a western-blot assay (**d**). An inset shows fibrils from a positive control, an  $A\beta$  fibril solution of 0.1mg.mL<sup>-1</sup>. Scale bars, 100 nm.

**Arrayed and high-throughput format for systematic analysis.** To demonstrate the capability of a high-throughput and systematic analysis, we prepared 200 devices and ran all of the assays using materials from the same batch. Each plate included twenty-five  
60 devices with individual  $A\beta$  environments and eight plates were prepared at the same time (Fig. S3).

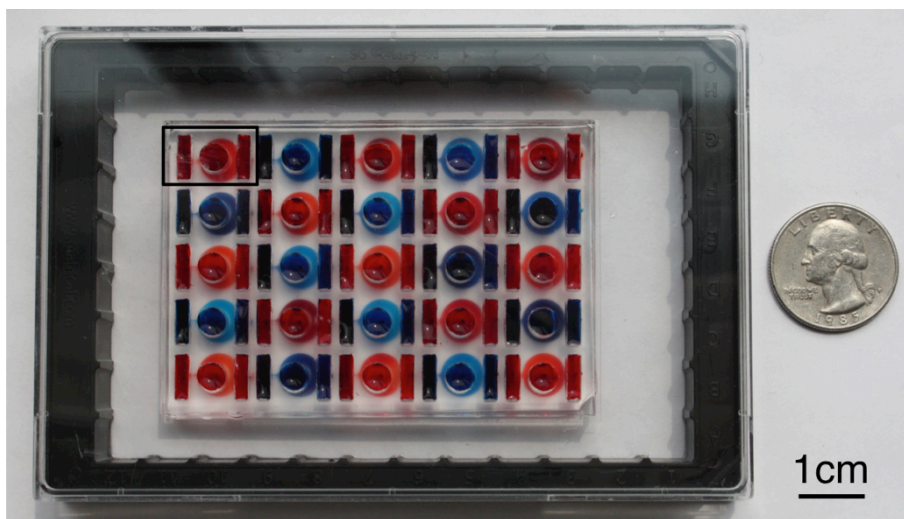


**Figure S3. A photo of arrayed devices.** Individual conditions are constructed on a large scale. An image in a square represents a single platform.

65 **Microglial recruitment with time.** To compare the roles of  $sA\beta$  in various forms and  
doses on microglia migration with time, we measured the microglia recruitment index  
every two days (**Fig. S4**). We found that the activation of microglia by  $sA\beta$  was more  
effective and faster when  $sA\beta$  was present in a monomeric ( $R.I.=5.0$ ) compared to an  
oligomeric form ( $R.I.=4.0$ ) at day 8 after exposure probably due to the fast diffusion of the  
70 smaller monomers. Also, the peak activity at two concentrations at 23  $\text{pg.mL}^{-1}$  and 23  
 $\text{ng.mL}^{-1}$  became discernible with time.

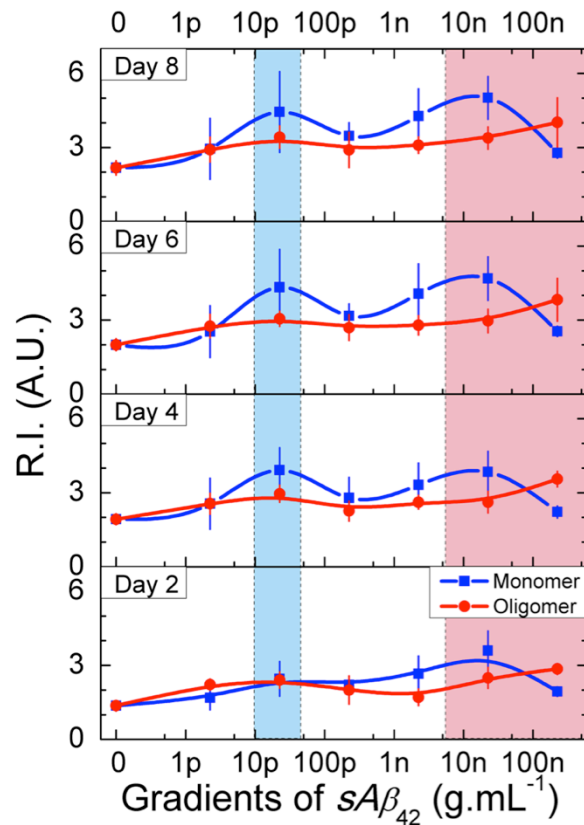


**Figure S4. Gradual recruitment of microglia toward the sources of soluble  $A\beta$ .**

**Microglial co-localization.** Microglial co-localization on surface-bound  $A\beta$  (i) was  
75 evaluated by counting number of microglia (ii) overlapped with patterned surface-bound  
 $A\beta_{42}$  (iii) on wells (Fig. S5) and in microfluidic platforms supplying gradients of soluble  
 $A\beta_{42}$  (Fig. S6).

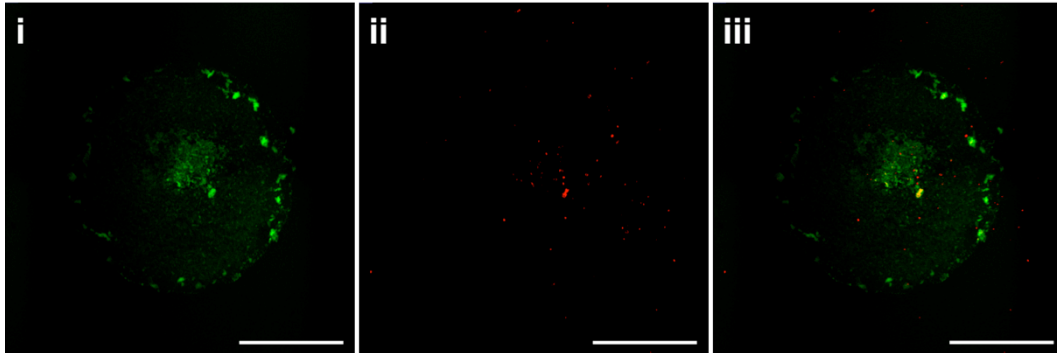


**Figure S5.** The co-localization of microglia on surface-bound  $A\beta$ . Scale bars, 1 mm.

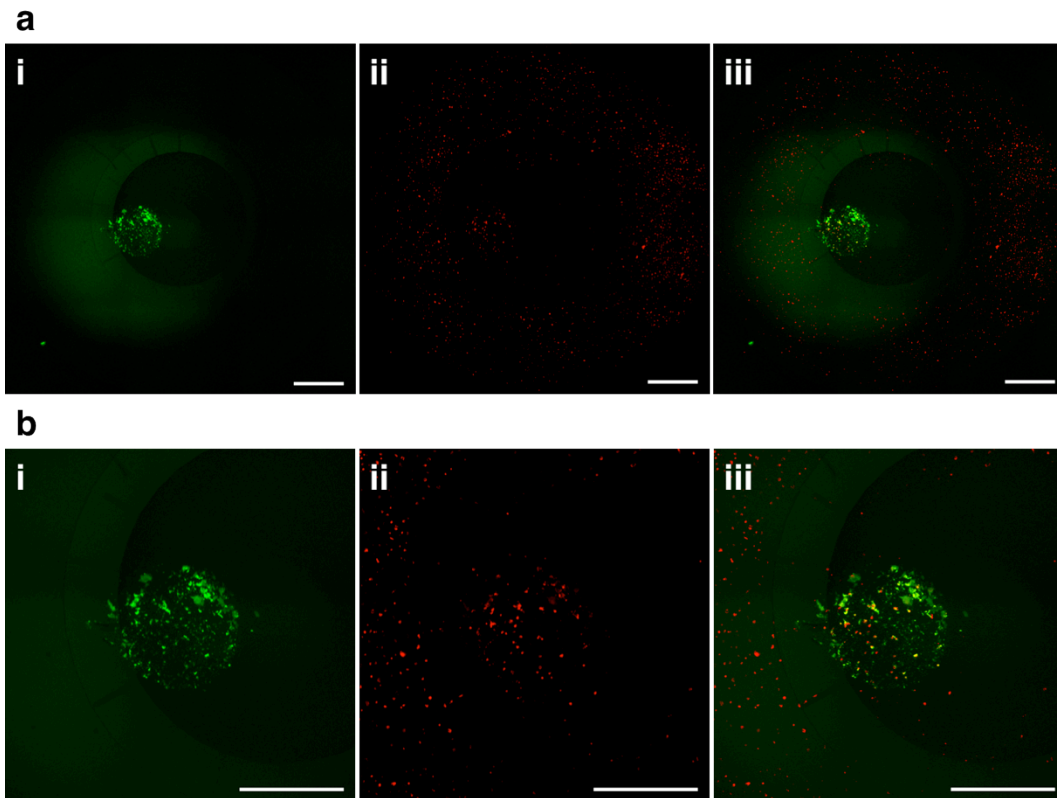


**Figure S6.** The accumulation of microglia on surface-bound  $A\beta$  in the combination of a gradient of soluble  $A\beta$ . Scale bars, 1 mm.



## Supplementary Methods

80 **Soluble  $A\beta$  preparation.** We prepared soluble  $A\beta$  monomer by dissolving a synthesized clear human  $A\beta$ , 1-42 (4349-v, Peptide Institute, Inc., Japan) and a FITC-labeled human  $A\beta$ , 1-42 (A-1119, rPeptide, Bogart, GA, USA) in DMSO at  $1 \text{ mg.mL}^{-1}$  for a monomer form. We skipped the usual HFIP pretreatment and directly dissolved  $A\beta$  in DMSO following the guideline from the company that synthesized the  $A\beta$  peptides (Peptide Institute, Inc., Japan).  
85 Even though  $A\beta$  pretreatment in HFIP is generally considered, the issue of the HFIP toxicity was recently raised by Capon *et al*<sup>1</sup>. Also, the slow evaporation of HFIP may trigger the formation of  $A\beta$  oligomers, which could hasten fibril formation in combination with the humidity in air. The dissolved  $A\beta$  monomer solution was further diluted in PBS at  $0.1 \text{ mg.mL}^{-1}$  and incubated for a week at  $4 \text{ }^\circ\text{C}$  or in a shaker at  $37 \text{ }^\circ\text{C}$  to prepare oligomeric  
90 and fibrillar forms, respectively.

**Surface-bound  $A\beta$  preparation.** We prepared bound  $A\beta$  using physisorption of soluble  $A\beta$  on a PLL coated surface. To form a uniformly coated bound  $A\beta$  fibril, soluble  $A\beta$  fibrillar solution was dropped on a PLL-coated glass-bottomed 24 well plate (P24G-1.5-13-F,  
95 MatTek Corp., Ashland, MA, USA) and dried in a vacuum chamber at a room temperature. To pattern bound  $A\beta$ , a PDMS stencil with 1 mm holes (HT 6240 machined by the laser machine) was placed on the PLL-coated glass and  $2 \text{ } \mu\text{L}$  of soluble  $A\beta$  oligomeric/fibrillar solutions were dropped and dried at  $4/37 \text{ }^\circ\text{C}$ , respectively.

100 **Immunoblotting.** SDS-PAGE was performed as previously described<sup>2</sup> with some modifications.  $A\beta$  monomers and oligomers without or with incubation were

electrophoresed on 4-12 % NuPAGE gel (Invitrogen) in MES SDS running buffer (Invitrogen). Gels were transferred to nitrocellulose membrane (Protran, Whatman, Kent, UK), and blocked for 30 min at RT in 5% non-fat skim milk/TBST (Tris-buffer saline with 0.1% Tween20). Membranes were probed with  $0.2 \mu\text{g.mL}^{-1}$  of monoclonal anti- $A\beta$  antibody 6E10 (Signet, Dedham, MA, USA) for 12 hours at 4 °C. Following incubation with horseradish peroxidase conjugated secondary anti-mouse antibody (Bio-Rad Life Science, Hercules, CA, USA) for 1 hour at RT, immunoreactive proteins were developed using ECL kit (Western Lightning, PerkinElmer, Waltham, MA, USA) and detected on Hyperfilm ECL (GE Healthcare Life Sciences). The samples were derived from the same experiments and blots were processed in parallel.

**Sandwich ELISA.** The total amounts of  $A\beta$  was quantified as previously described<sup>2</sup>. Soluble  $A\beta$  samples were incubated with 8 M guanidine-HCl (concentration of guanidine-HCl in the sample is 4 M) for 30 min at RT to dissociate  $A\beta$  oligomers to monomers<sup>3</sup> and diluted by 7 volumes of standard dilution buffer (final concentration of guanidine-HCl in the sample is 0.5 M). After dilution, samples were subjected to BNT77/BC05 for a human  $A\beta_{42}$  ELISA kit (Wako chemicals, Richmond, VA, USA). The fraction of  $A\beta$  oligomers was quantified using a human  $A\beta_{42}$  oligomer-specific ELISA kit (82E1-specific, Immunobiological laboratories, MN, USA) as suggested by the manufacturer without pre-treatment by quinidine-HCL.

**Negative Stain Electron Microscopy.** Samples were spread on carbon film on nickel grids (Electron Microscopy Sciences, Hatfield, PA, USA), negatively stained with 2% (w/v) phosphotungstic acid, pH 7.0 (Sigma-Aldrich), and viewed in an electron microscope (JEOL-1011, JEOL USA, Inc., Boston, MA, USA)<sup>4</sup>. Magnification, x80k. HV, 80 kV.

**Multi-cytokine assay.** A panel of 27 human cytokines was measured by using a human 27-plex kit (Cat No. M50-0KCAF0Y, Bio-Rad, Hercules, CA, USA) and read out on the Bio-Plex 200 instrument (Cat No. 171-000201, Bio-Rad), as shown in Figure 3a. Instrument readouts were calibrated to a serial dilution standard curve prepared according to the protocols suggested by the manufacturer. MCP-1 was re-measured after a 1:8 dilution in culture media using the MCP-1 single-plex (Cat. No. 171-B5021M, Bio-Rad), read out on the Bio-Plex 200-instrument, calibrated against a serial dilution standard curve of MCP-1 compound (Cat. No. 279MC, R&D Systems, Inc., Minneapolis, MN, USA), as shown in Figure 3c.

**Analysis of cellular motility.** To automatically count the microglia cells, we used the open-sourced software, CellProfiler (Broad Institute, Boston, MA, USA) The cellular spatial location inside devices was utilized to calculate the fraction of cells and R.I. by using a programmable engineering language, Matlab (MathWorks, Inc, Natick, MA, USA). To track the migration of individual cells, we employed MetaMorph (SPOT Imaging Solutions, Sterling Heights, MI, USA). The number of cells on bound  $A\beta$  was counted manually in order to avoid artifacts due to the strong absorption of the microglia staining dye to the sticky bound  $A\beta$ .

**Recruitment index.** Microglia recruitment by soluble  $A\beta$  was quantified by comparing the fraction of cells inside the central compartment to the total number of cells in the corresponding device (**Fig. S7**). The fraction,  $\alpha_{rec}$ , is calculated as  $\alpha_{rec} = N_{cent} / N_{tot}$ , where  $N_{cent}$  is the number of cells in the central compartment and  $N_{tot}$  is the number of cells in the device (inside and outside the central compartment). The recruitment index,  $R.I.$ , is obtained by normalizing the fraction calculated each day with the fraction at ‘day 0’.

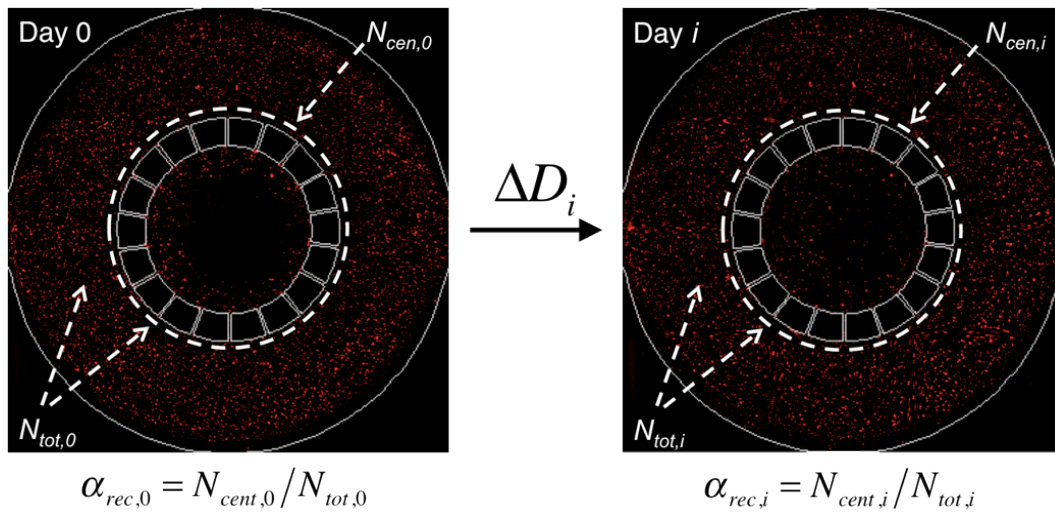


**Figure S7. Schematic representation for the definition of the recruitment index,  $R.I.$**

**Localization index.** Microglia localization on the patterned  $A\beta$  was quantified by counting the cells in the patterned area (**Fig. S8**). The localization index,  $L.I.$ , is obtained by normalizing the number of cells on the patterned  $A\beta$  of each day with the number of cells of ‘day 0’.

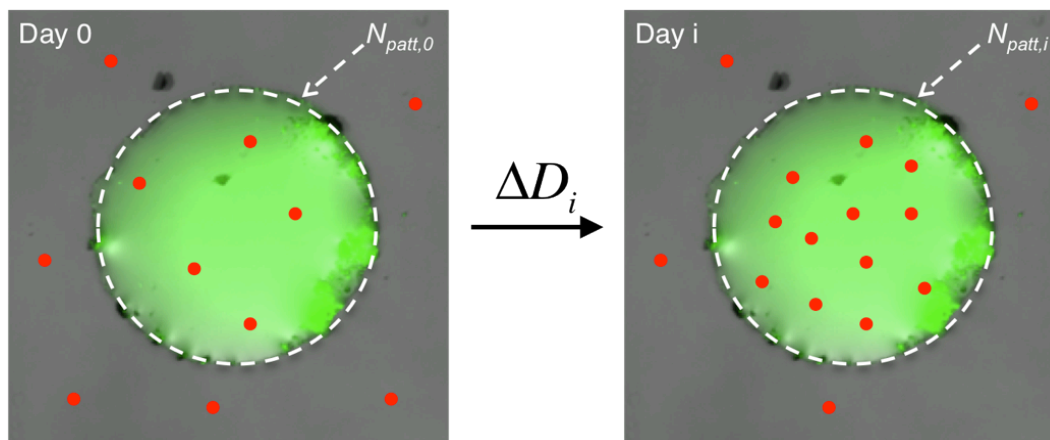


**Figure S8. Schematic representation for the definition of the localization index,  $L.I.$**

### Movie Legends

160 **Movie S1.** This movie shows a directional migration of microglia along a gradient of  $sA\beta$  monomers at  $2.3 \text{ ng.mL}^{-1}$ . The images were taken every hour for four days with x10 magnification lens and plays 36,000 times faster than an original speed. Avi format. 1.3 MB.

165 **Movie S2.** This movie shows random navigation of microglia in the absence of a gradient of  $sA\beta$ . The images were taken every hour for four days with x10 magnification lens and plays 36,000 times faster than an original speed. Avi format. 1.2 MB.

**Movie S3.** This movie shows microglial clearance of  $A\beta$ -like particles on  $A\beta$  fibrils coated glass surface. The images were taken every 20 minutes for four days with x10 magnification lens and plays 36,000 times faster than an original speed. Avi format. 2.5  
170 MB.

**Movie S4.** This movie shows microglial clearance of a dead cell. The images were taken every 20 minutes for four days with x10 magnification lens and plays 36,000 times faster than an original speed. Avi format. 1.5 MB.

175 **References**

1. Capone, R. et al. Amyloid- $\beta$ -Induced Ion Flux in Artificial Lipid Bilayers and Neuronal Cells: Resolving a Controversy. *Neurotox Res* **16**, 1–13 (2009).
2. Hashimoto, T. et al. Apolipoprotein E, especially apolipoprotein E4, increases the oligomerization of amyloid beta peptide. *J. Neurosci.* **43**, 15181–15192 (2012).
- 180 3. Yamada, K. et al.  $A\beta$  immunotherapy: intracerebral sequestration of  $A\beta$  by an anti- $A\beta$  monoclonal antibody 266 with high affinity to soluble  $A\beta$ . *J. Neurosci.* **29**, 11393–11398 (2009).
4. Hori, Y. et al. The Tottori (D7N) and English (H6R) Familial Alzheimer Disease Mutations Accelerate  $A\beta$  Fibril Formation without Increasing Protofibril Formation. *J.*  
185 *Biochem.* **282**, 4916–4923 (2007).